# The Influence of Hot Compression on the Surface Characteristics of Poplar Veneer

Wending Li, Chao Wang, Yang Zhang,* Chong Jia, Chenchao Gao, and Juwan Jin

The surface characteristics of wood veneer are inevitably influenced by hot compression treatment, which is crucial to bonding ability in the production of veneer-based composites such as plywood and laminated veneer lumber (LVL). The objective of this study was to investigate the effect of compression at the temperature of 120 °C on the surface roughness, surface element compositions, and surface free energy (SFE) of poplar veneer. The results showed that the surface roughness of veneer decreased with increasing compression ratio (CR). X-ray photoelectron spectroscopy (XPS) analysis indicated that the oxygen to carbon atoms ratio (O/C ratio) of the veneer surface decreased, while the carbon C1 to C2 atoms ratio (C1/C2 ratio) increased due to hot compression. The SFE of veneer increased by 12% at the CR level of 11%. The improvement in wettability was mainly due to the interfacial contact area increase of the hydrophilic veneer and the decrease in hydrophobic air in the liquid-veneer interface as the CR level increased.

*Keywords: Surface free energy; Contact angle; Veneer; Hot compression; Surface roughness; X-ray photoelectron spectrometer (XPS)*

*Contact information: College of Materials Science and Engineering, Nanjing Forestry University, Nanjing, P. R. China 210037; *Corresponding author: yangzhang31@126.com*

## INTRODUCTION

Wood is a complex hygroscopic material, composed of cellulose, hemicellulose, lignin, and extractives. It has a heterogeneous, rough, or even porous surface due to the cell wall structure (Inari *et al.* 2006; Mohammed-Ziegler *et al*. 2004).

As one of the most important fast-growing tree species in China, poplar (*Populus euramericana* cv. *'I-214'*) trees have been widely planted and provide raw materials for making fiberboard, particleboard, plywood, and nonstructural laminated veneer lumber (LVL). But poplar wood is a challenging species for engineered wood products due to its lower wood quality, including intrinsic low specific gravity and poor mechanical properties (Bao and Liu 2001; Cai *et al*. 2013; Wei *et al*. 2013; Zhang *et al.* 2012). To overcome these drawbacks, wood densification by hot compression has been shown to be a promising modification technique (Fang *et al*. 2012b; Gong *et al*. 2010). During the hot compression process, wood density is increased by reducing the void volume of the lumens, and hence the physical and mechanical properties can be enhanced significantly (Kutnar *et al*. 2009; Kutnar and Kamke 2012; Rautkari *et al*. 2010). Densified wood as a patent product dates back to the 1900s in America (Fang *et al*. 2012b; Haygreen and Daniels 1969). Since then, many researchers have studied the effect of the wood densification process on mechanical properties (Anshari *et al*. 2011; Avila *et al*. 2012; Fang *et al*. 2012a; Heräjärvi 2009), set recovery (Fang *et al*. 2011; Rautkari *et al*. 2010), and surface hardness (Bao and Liu 2001; Gong *et al*. 2010).

Set recovery of compressed wood due to internal stresses can be almost eliminated by a high-temperature hydrothermal treatment (above 200 °C) (Fang *et al*. 2011; Rautkari *et al*. 2010). However, hot compressed wood with a higher temperature (above 160 °C) increases the hydrophobic character of the wood surface due to the migration of extractives and the cleavage of acetyl groups of hygroscopic compounds such as hemicellulose (Büyüksarı 2013; Diouf *et al*. 2011; Tjeerdsma and Milit 2005). The wettability of the wood surface decreases significantly with an increase of hot compression temperature (Ayrilmis *et al*. 2009). For wood that is heat-treated below 120 °C, the extractives are minimally affected and the wood surface remains totally hydrophilic (Hakkou *et al*. 2005; Poncsak *et al*. 2009).

Compression treatment at a relatively low temperature mainly influences the surface quality of wood or veneer by varying the surface morphology at a nanometric and micrometric scale (Candan *et al*. 2010; Miller *et al*. 1996; Ostrovskaya *et al*. 2003). The lathe checks of veneer can be conglutinated, and the surface roughness was reported to be decreased by the compression process (Fang *et al*. 2012b). İmirzi *et al*. (2014) studied the effect of temperature of compression on the surface roughness of Scots pine and found that the lowest roughness was obtained at 140 °C. Bekhta *et al*. (2009, 2012) used the compressed veneer to produce higher shear strength plywood with lower glue consumption and lower pressing pressure. They also found the temperature of veneer compression had a significant effect on the shear strength of plywood. However, there is a lack of information about the surface chemical structure and elemental composition of veneer during the process of compression.

The surface qualities of veneer are crucial to surface wettability and bonding quality between veneer sheets. Wettability can be characterized using thermodynamic wetting parameters such as contact angle (CA), surface free energy (SFE), and work of adhesion (WA) (Wålinder 2002). SFE is an important parameter in evaluating the chemical properties of solid materials surface. It reflects the state of imbalance in intermolecular interactions at the phase boundary of two mediums and represents the wettability of the solid materials (Čern *et al*. 2008). It is increasingly used as a measure of adhesive properties in the area of wood-based composites (Rudawska and Jacniaka 2009).

To date, numerous investigations of the SFE of wood have been reported, including SFE and its components (Gardner 1996; Ma *et al*. 1990; Shen *et al*. 1998; Shi and Gardner 2001; Wålinder and Ström 2001), differences within and between wood species (McConnell and Shi 2011; Mohammed-Ziegler *et al*. 2004; Rossi *et al*. 2012), heat treatment (Kutnar *et al*. 2008; Wålinder 2002), and comparison of different models (Gindl *et al*. 2001; Zenkiewicz 2007). Various models have been developed to calculate the SFE of a solid from CA measurements, including the critical surface tension approach (Mahadik *et al*. 2011; Zisman 1963), harmonic mean equation (Wu 1971), geometric mean equation (Owens and Wendt 1969), and acid-base approach (Van Oss *et al*. 1987; Van Oss and Giese 1995). Compared to other approaches, the acid-base approach provides greater accuracy in calculating SFE components of wood (Gindl *et al.* 2001).

Currently, despite some studies related to the surface roughness of compressed veneer (Bekhta *et al*. 2009, 2012; Fang *et al*. 2012b), there is still insufficient information concerning the surface characteristics of veneer under the process of hot compression, which directly influence the bonding quality of veneer-based composites. Therefore, the objective of this work was to investigate the impact of hot compression treatment at a temperature of 120 °C on the surface roughness, surface element composition, and SFE

of poplar veneer to provide a guide for the appropriate application of compressed veneer in veneer-based composites.

## EXPERIMENTAL

### Materials

Seven-year-old green poplar (*Populus euramericana* cv. 'I-214') logs were obtained from Jiangsu province, China. Eight logs (about 50 cm in length and 20 cm in diameter) from each of five different trees were used for veneer cutting with a laboratory rotary lathe. All veneer were air-dried for 7 days to reach an approximate moisture content of 15% and a density of approximately 0.41 g $cm^{-3}$. Five sheets of veneer were selected randomly, and each one was sawn to a smaller sheet with dimensions of 120 mm (length) × 50 mm (width) × 3.2 mm (thick). Each veneer sheet was tailored to six strips with a length of 50 mm and a width of 20 mm, as shown by the schematic (Fig. 1). The veneer strips were conditioned in a climate chamber with a relative humidity (RH) of 65% and a temperature of 20 °C for one month to reach equilibrium moisture content prior to compression.

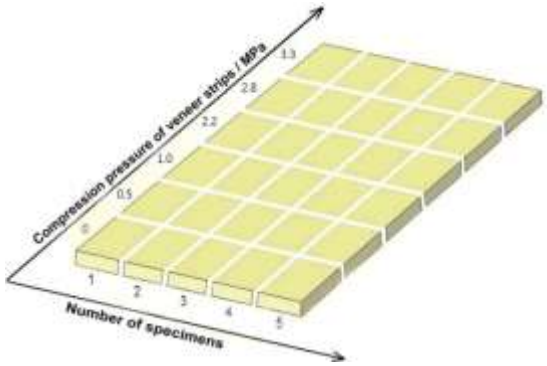


**Fig. 1.** Schematic illustration of the preparation for veneer specimens

### Methods

*Compression treatment*

Veneer strips were compressed by a laboratory hot-press for 15 min. The hot pressing temperature was 120 °C (a normal temperature used in the production of veneer-based composites). Based on our previous research (Li *et al.* 2010; Zhang *et al.* 2012), the pressure levels were set at 0.5, 1.0, 2.2, 2.8, and 3.3 MPa. The compression ratio (CR) was calculated according to Eq. 1,

$$CR = \frac{T_0 - T_C}{T_0} \times 100\% \quad (1)$$

where $T_0$ and $T_C$ are the thicknesses of the specimen before and after the compression treatment, respectively. Meanwhile, non-compressed veneer strips, which were used as control specimens, were placed in an oven at 120 °C for 15 min.

Then, each strip was cut into five specimens with a length of 20 mm and width of 10 mm (Fig. 1). Five replicates per treatment were prepared (5 specimens × 6 treatments × 5 replicates; n = 150). The actual dimensions of the specimens were measured three times using a caliper (precision 0.01 mm) immediately after treatment.

*Roughness measurements*

The average roughness ($R_a$) and average maximum height of the profile ($R_z$) are defined in the ANSI/ASME standard (B46.1 2002). A TR110 Roughometer (TIME GROUP, China) with a display resolution of 0.01 μm was used to evaluate the roughness. Immediately after hot compression, five locations on each specimen were randomly selected and measured from both the tight side and loose side. The cutoff length was 0.8 mm, and the evaluation length was 4.0 mm. The overall veneer roughness parameter $R_a$ was the arithmetic mean of $R_a$ values from both the tight side and the loose side. The roughness parameter of $R_z$ was measured following the same routine.

*X-ray photoelectron spectroscopy*

A PHI VersaProbe 5000 Scanning X-ray photoelectron spectrometer (XPS; ULVAC-PHI, Inc., Japan) was used to identify the elements and chemical data present at the surface of the specimens. The specimens with an area of 5 mm × 5 mm were placed in the chamber. The base vacuum in the chamber was below $6.7 \times 10^{-10}$ mbar. X-rays were irradiated from a monochromatic Al Kα source (1486.6 eV) operating at 40 W at an incident angle of 45°. Carbon C1s peaks with high-resolution spectra at 285 eV were corrected. A Gaussian function was used to curve fit the spectrum using PeakFit, v4.12 (SeaSolve Software Inc., USA). The C1/C2 ratios were determined according to peak area.

*Contact angle measurements*

The Wilhelmy plate method was used to measure the CA of prepared veneer specimens with various liquids (Table 1). The tests were carried out using a Sigma 701 tensiometer (KSV, Finland). Each specimen was suspended from the electronic microbalance (precision 1.0 μN) and was immersed and withdrawn from a probe liquid at a constant velocity of 5 mm $min^{-1}$. The whole process was completed in a closed environmental chamber at 20 °C and RH 50%. The specimens were tested in both polar and nonpolar probe liquids (Table 1): water (distilled in laboratory); formamide (99.0% purity, Sinopharm Inc., Shanghai); glycerol (99.0% purity, Nanjing Chemical Inc., Nanjing); diiodomethane (chemically pure, Sinopharm Inc., Shanghai), and n-hexane (97.0% purity, Sinopharm Inc., Shanghai). Five replicates were tested for each probe liquid.

**Table 1.** Density, Viscosity, Surface Tension, and Surface Tension Components of Probe Liquids at 20 °C

| Test liquids | Density (g $cm^{-3}$) | Viscosity (mPa. s) | $(\gamma_L)^b$ (mJ $m^{-2}$) | $(\gamma_L^{LW})^c$ (mJ $m^{-2}$) | $(\gamma_L^-)^d$ (mJ $m^{-2}$) | $(\gamma_L^+)^e$ (mJ $m^{-2}$) |
|---|---|---|---|---|---|---|
| Water (W)[a] | 0.999 | 1.002 | 72.8 | 21.8 | 25.5 | 25.5 |
| Formamide (F)[a] | 1.133 | 2.93 | 58 | 39 | 2.28 | 39.6 |
| Glycerol (G)[a] | 1.250 | 1499 | 64 | 34 | 3.9 | 57.4 |
| Diiodomethane (D)[a] | 3.325 | 3.35 | 50.8 | 50.8 | 0 | 0 |
| n-Hexane (H)[a] | 0.663 | 0.29 | 18.4 | 18.4 | 0 | 0 |

[a] Abbreviations represent probe liquids; [b]surface tension of probe liquids; [c]Lifshitz-van der Waals component; [d]electron-donor parameter; [e]electron-acceptor parameter. Data is referenced from Good 1992, Van Oss *et al*. 1992, Kwok *et al*. 1994, Shen *et al*. 1998, and McConnell and Shi 2011.

*Surface free energy determination*

The general equation describing the interaction of surface tension of a liquid (*L*) and a solid (*S*) is the Young equation (Young 1805), given as Eq. 2:

$$\gamma_L \cos\theta = \gamma_S - \gamma_{SL} \quad (2)$$

Here, $\gamma_L$ is the surface tension of test liquid, $\theta$ is the CA, $\gamma_S$ is the SFE of the solid, and $\gamma_{SL}$ is the solid-liquid interfacial tension (Van Oss *et al*. 1992).

The concept of work of adhesion ($W_{SL}^a$) is introduced, which represents the work needed to separate an area of liquid from an area of solid (Good 1992; Selvakumar *et al*. 2010).

$$W_{SL}^a = \gamma_S + \gamma_L - \gamma_{SL} \quad (3)$$

The Young-Dupre equation is obtained by combining Eqs. 2 and 3 (Good 1992; Wålinder 2002):

$$W_{SL}^a = \gamma_L(1 + \cos\theta) \quad (4)$$

To obtain the total SFE and its components for the veneer surface, the acid-base approach was applied. The acid-base approach as proposed by Van Oss *et al* (1987) for the SFE of a solid has two parts:

$$\gamma = \gamma^{LW} + \gamma^{AB} \quad (5)$$

where $\gamma^{LW}$ and $\gamma^{AB}$ are the Lifshitz-van der Waals (LW) and Lewis acid-base (AB) energy components, respectively.

The surface tension component arising from the London dispersion force designates for LW energy component or apolar component. The AB energy component or polar component is mainly due to hydrogen bond interactions, dipole-dipole, and dipole-induced dipole force (Good 1992; Kwok *et al*. 1994). $\gamma^{AB}$ can be expressed in terms of the products of its electron-acceptor (Lewis acid) and electron-donor (Lewis base) parameters (Van Oss *et al*. 1987; Van Oss and Giese 1995),

$$\gamma^{AB} = 2\sqrt{\gamma^+}\sqrt{\gamma^-} \quad (6)$$

where $\gamma^+$ is the electron-acceptor parameter and $\gamma^-$ is the electron-donor parameter.

The SFE component $\gamma^{LW}$ and polar parameters $\gamma^+$ and $\gamma^-$ of a solid (*S*) can be calculated by CA determination with one apolar and at least two polar probe liquids (*L*), using the following equation (Kwok *et al*. 1994),

$$(1 + \cos\theta)\gamma_L = 2\sqrt{\gamma_S^{LW}\gamma_L^{LW}} + 2\sqrt{\gamma_S^+\gamma_L^-} + 2\sqrt{\gamma_S^-\gamma_L^+} \quad (7)$$

*Statistical analysis*

A one-way analysis of variance (ANOVA) was performed by using the SPSS software (Version 19.0, IBM SPSS Inc., Chicago, USA) for data analysis. The

differences between means were tested with least significant differences (LSD) at 5% level.

## RESULTS AND DISCUSSION

### Effect of Compression Ratio on Surface Roughness

The resulting CR for each specimen is listed in Table 2. The surface roughness parameters $R_a$ and $R_z$ for non-compressed (control specimen) and compressed veneer are shown in Fig. 2.

**Table 2.** Compression Ratios of Veneer

| Specimen No. | Compression pressure (MPa) | CR (%) |
|---|---|---|
| Control | 0 | 0 |
| CR2 | 0.5 | 2 |
| CR5 | 1.0 | 5 |
| CR11 | 2.2 | 11 |
| CR34 | 2.8 | 34 |
| CR45 | 3.3 | 45 |

Compared with the control, both values of $R_a$ and $R_z$ decreased drastically from 5.01 µm and 30.09 µm to 4.23 µm and 23.88 µm for specimen CR11, respectively. Then, the $R_a$ and $R_z$ values decreased gently to 3.41 µm and 20.0 µm, respectively, at a CR level of 45%. Analysis of variance (ANOVA) confirmed the effects of CR on $R_a$ and $R_z$ were both significant ($P < 0.05$).

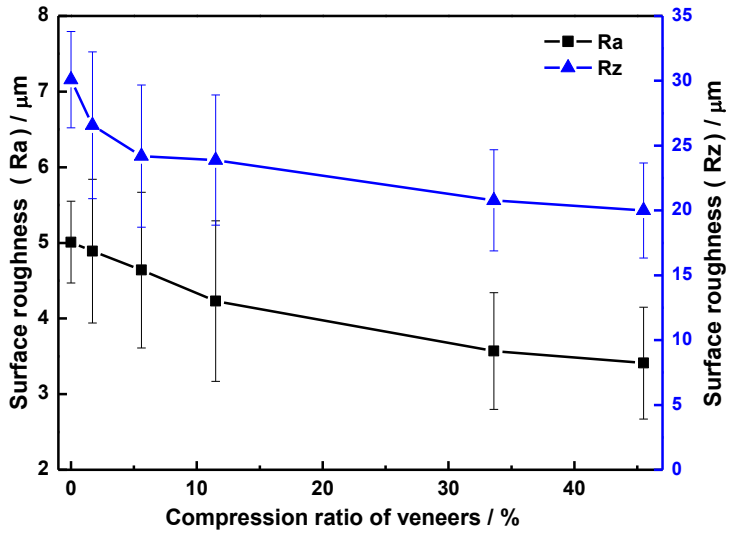


**Fig. 2.** The effect of CR on surface roughness of veneer

The rough and porous structure of the veneer surface is caused by the cell lumens and lathe checks. The pore size distribution of lumens can be distinguished with diameters in ranges of 0.5 to 58 µm (macropores), 80 to 500 nm (mesopores), and 1.8 to

80 nm (microspores) (Plötze and Niemz 2011), while the depth of lathe checks caused by rotary cutting can reach the millimeter scale. Consequently, the decreasing surface roughness may be related to the reduction of void space and conglutination of lathe checks under pressure during veneer compression (Fang *et al*. 2012b).

## XPS Analysis

Figure 3 presents the typical C1s and O1s wide XPS survey spectrum and C1s high-resolution spectrum of air-dried, control, and CR45. Surface element composition results are shown in Table 3.

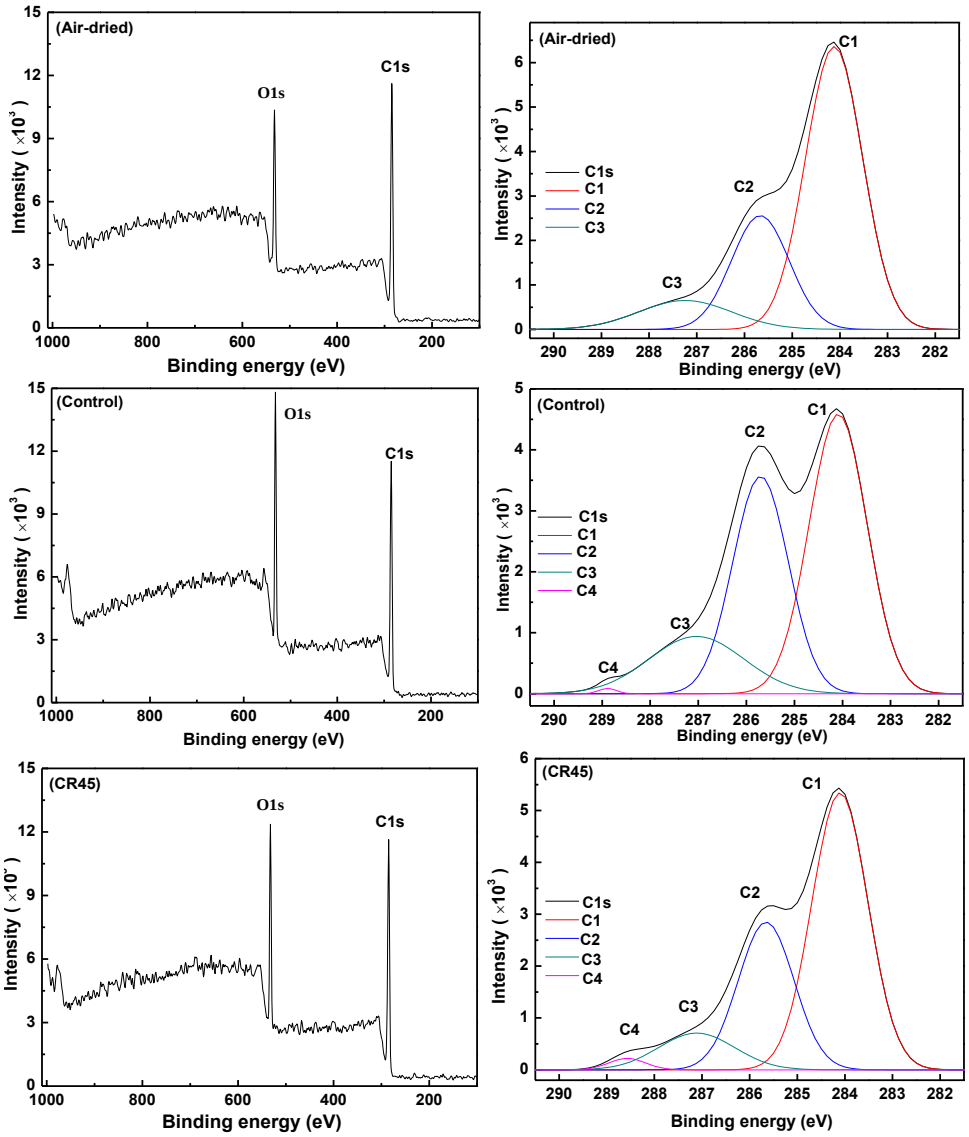


**Fig. 3.** XPS spectrum (left) and C1s high-resolution spectrum (right) of specimens

C1 is related to carbon-carbon and carbon-hydrogen bonds in extractives and lignin. C2 can result from all three classes of wood components, but predominantly in the carbohydrates as -CHOH and in lignin as β-ether and -COH bonds (Sernek 2002; Young *et al*. 1982). It was clear that the atomic composition and C1s components of veneer

specimens differed strongly. The O/C ratio of veneer surface increased from 0.27 under air-dried to 0.41 under oven-dried (control) specimens. Conversely, the C1/C2 ratio decreased from 2.46 to 1.34. The increased O/C ratio can be attributed to the evaporation and removal of water-insoluble extractives (such as terpenoids, fats, fatty acids, glycerides, and wax) present in the surface of veneer (Inari *et al*. 2006). The decrease of the C1/C2 ratio provides additional information to support the interpretation. This is consistent with the results in previous studies (Diouf *et al*. 2011), which used a much higher temperature of 160 °C. Wood extractives are hydrocarbons or their derivatives which are mostly hydrophobic. Consequently, removal of the extractives of veneer surfaces by oven-drying at 120 °C may contribute to its wettability.

**Table 3.** Surface Atomic Percentages, O/C ratio, and C1s Distribution of Specimens by XPS Analysis

| Specimens | Atomic composition (%) | | | C1s component (%) | | | | |
|---|---|---|---|---|---|---|---|---|
| | C | O | O/C | C1 | C2 | C3 | C4 | C1/C2 |
| Air-dried | 78.3 | 21.7 | 0.27 | 63.6 | 25.8 | 10.6 | 0 | 2.46 |
| Control | 70.8 | 29.2 | 0.41 | 48.0 | 35.7 | 16.1 | 0.3 | 1.34 |
| CR45 | 75.0 | 25.0 | 0.33 | 57.6 | 30.5 | 10.4 | 1.6 | 1.88 |

Compared to the control specimen, the O/C ratio of specimen CR45 decreased slightly, dropping to 0.33. The C1 component increased to 57.6%, while the C2 component decreased to 30.5%. Since the preferential degradation of hemicellulose is above 120 °C, there was nearly no chemical degradation on veneer surfaces under compression treatment at 120 °C. This indicates that the migration and concentration of extractives to the veneer surfaces may lead to the chemistry change of the surface. Some researchers report (Hakkou *et al*. 2005; Sernek 2002) that the changes in surface chemistry can also be related to some rearrangement of surface lignin, which is an amorphous and glassy polymer. The driving force for reorientation is thermodynamic, when a surface tends to minimize its free energy. In any event, either of them has a negative effect on the wettability of veneer surface.

## Contact Angles and Work of Adhesion for Veneer-Liquid Interaction

The instant advancing CAs for probe liquids on the compressed veneer and the control are provided in Table 4. Basically, the determined CA values for all probe liquids except hexane show a decreasing tendency with an increase CR level of veneer. Due to the low viscosity and low surface tension of hexane, the advancing liquid front wicks along the veneer surface much faster than the immersion velocity. So the determined CAs were not for the probe liquids on veneer surface, but rather on the veneer-liquid interface called the monolayer film adsorbed by the veneer surface. The adsorbed monolayer is sufficient to change the surface properties of veneer (Wålinder and Ström 2001; Zisman 1963) and can be easily wetted. Consequently, all the measured CAs for hexane were zero (Table 4).

**Table 4.** Instant Advancing CAs for the Control and Compressed Veneer Surfaces with Respect to Each Probe Liquid (20 °C)

| Specimen No. | CR (%) | CA (degrees) | | | | |
|---|---|---|---|---|---|---|
| | | Water | Formamide | Glycerol | Diiodomethane | Hexane |
| Control | 0 | 97.8(8.2)$^{a}$ | 74.9(2.8)$^{a}$ | 121.2(4.3)$^{a}$ | 47.1(1.9)$^{a}$ | 0(0) |
| CR2 | 2 | 88.5(5.2)$^{b}$ | 68.7(5.6)$^{b}$ | 120.6(3.9)$^{a}$ | 46.8(3.0)$^{a}$ | 0(0) |
| CR5 | 5 | 87.9(3.7)$^{b}$ | 66.9(3.3)$^{b}$ | 119.9(2.4)$^{a}$ | 42.8(2.2)$^{b}$ | 0(0) |
| CR11 | 11 | 85.5(4.1)$^{b}$ | 62.6(4.8)$^{c}$ | 116.3(2.0)$^{b}$ | 41.4(1.2)$^{bc}$ | 0(0) |
| CR34 | 34 | 83.5(3.5)$^{b}$ | 61.6(4.7)$^{cd}$ | 115.1(3.9)$^{bc}$ | 40.4(1.5)$^{c}$ | 0(0) |
| CR45 | 45 | 82.3(3.3)$^{b}$ | 58.3(5.2)$^{d}$ | 112.7(1.6)$^{c}$ | 40.7(0.9)$^{c}$ | 0(0) |

Standard deviations are based on five replicates. Means with the same superscript letters in the same column are not significantly different at α = 0.05 using LSD.

The work of adhesion (WA) for veneer-liquid interactions is calculated from Eq. 4 and presented in Fig. 4. Clearly, compared to the control specimens, all of the WA values for water, formamide, glycerol, and diiodomethane showed a significant increase ($P < 0.05$) of CR at 11%. All WA values then increased slightly from a CR of 11% to 45%. The reason for this may be attributed to the air trapped in the rough and porous structure of the veneer surface which can decrease the veneer-liquid contact area (Čern *et al*. 2008; Selvakumar *et al*. 2010). With an increase of CR, the surface roughness decreases, which subsequently increases the WA. The WA values for the veneer-hexane interaction remains constant at 36.8 mJ m$^{-2}$ due to the zero CAs.

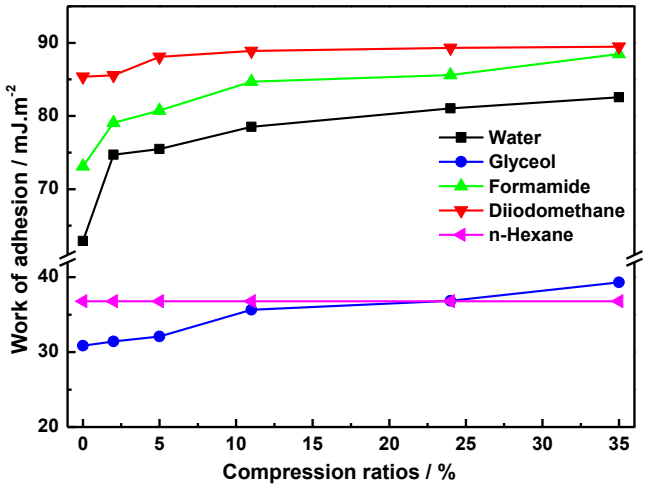


**Fig. 4.** The effect of CR on work of adhesion

Diiodomethane is a nonpolar liquid with a high LW component of 50.8 mJ m$^{-2}$. The diiodomethane interacts with veneer mainly through dispersive interactions and shows higher work of adhesion. As polar liquids, water and formamide have a large dipole moment and a strong tendency for hydrogen bonding to the hydroxyl groups of veneer substance (Selvakumar *et al*. 2010). With the high viscosity of glycerol, the veneer-glycerol interaction is much lower due to the higher CA with veneer.

## Surface Free Energy and its Components

Figure 5 shows the total SFE ($\gamma_S$), LW energy component ($\gamma_S^{LW}$), and AB energy component ($\gamma_S^{AB}$) of veneer obtained by an acid-base approach. The values of $\gamma_S^{LW}$, acid ($\gamma_S^+$), and base ($\gamma_S^-$) parameters of veneer surface were calculated by using Eq. 7 to combine a set of three equations in terms of three CAs from water, formamide, and diiodomethane, respectively.

Compared to the control, both the values of $\gamma_S$ and $\gamma_S^{LW}$ increased by 12.0% and 8.4% for compressed veneer with 11% CR level, respectively. Then, both increased slightly to 40.7 mJ m$^{-2}$ and 39.4 mJ m$^{-2}$ at the CR level of 45%. It seems that compression treatment had a significant influence on the $\gamma_S^{LW}$ component of SFE due to the decreasing surface roughness of veneer. The LW energy component exhibited a predominant contribution to the SFE, which is one of the characteristics of typical polymers (Mohan *et al*. 2011; Shen *et al*. 1998). The high $\gamma_S^{LW}$ can be explained by the high interaction ability of the dispersive part of available carbon-oxygen and carbon-carbon bonds within the veneer. Nevertheless, the values of AB energy component, $\gamma_S^{AB}$, were relatively small in comparison with the contribution of the LW energy component, and changed little with increasing CR (Fig. 5). This does not mean that the AB energy component is less important. On the contrary, it refers to the interaction between hydroxyl groups of veneer and functional groups of adhesive by forming the hydrogen bond (Sernek 2002; Shen *et al*. 1998).

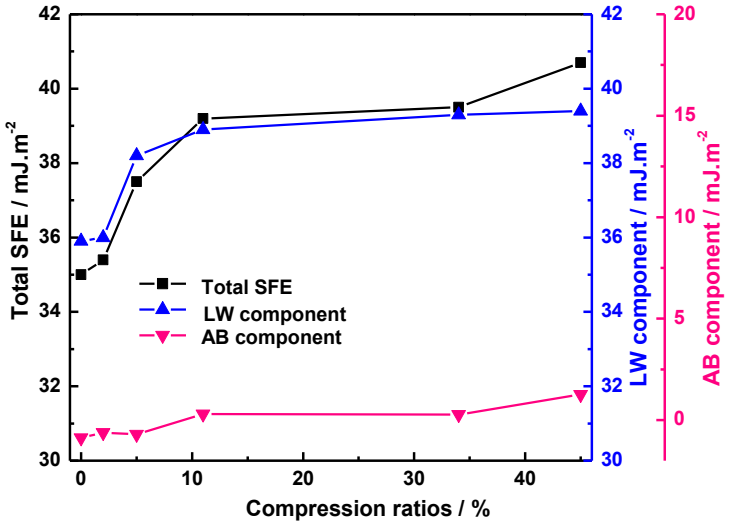


**Fig. 5.** The effect of CR on the total SFE and its components of veneer

Table 5 shows the acid ($\gamma_S^+$) and base ($\gamma_S^-$) parameters of veneer surfaces with different CR levels. It is evident from the data that the value of $\sqrt{\gamma_S^+}$ increased from -0.40 to 0.30, and the value of $\sqrt{\gamma_S^-}$ increased from 1.10 to 2.07. The acid-base properties of veneer are related to the functional groups on the veneer surface. The acid functionality is found in hydroxyl and/or acetyl groups, while the basicity comes from the carbonyl group (Ma *et al*. 1990; Shen *et al*. 1998). The base parameter of veneer surfaces is distinctly higher than the acid parameter, implying the veneer is monopolar basic. From the appearance of negative square roots values of $\sqrt{\gamma_S^+}$ arises a mathematical puzzle in solution of Eq. 7. So far, attempts to explain the physical meaning of it have not been convincing (Shen *et al*. 1999).

**Table 5.** Acid and Base Parameters of Veneer with Different CR Level

| Specimen No. | CR (%) | $\sqrt{\gamma_s^+}$ | $\sqrt{\gamma_s^-}$ |
|---|---|---|---|
| Control | 0 | -0.40 | 1.10 |
| CR2 | 2 | -0.16 | 2.00 |
| CR5 | 5 | -0.18 | 1.94 |
| CR11 | 11 | 0.08 | 1.93 |
| CR34 | 34 | 0.06 | 2.17 |
| CR45 | 45 | 0.30 | 2.07 |

Generally, the wettability of a solid surface is governed by the surface chemical composition and surface morphology (Mahadik *et al*. 2011; Shen *et al*. 1998). Here, the chemical changes on the veneer surfaces during the process of hot compression at 120 °C have a negative effect on its wettability. However, the effect is slight because almost no chemical degradation takes place at such a temperature.

An increase in CR levels results in a decrease of surface roughness, which contributes to the increase in SFE of the veneer. This phenomenon can be interpreted by the "lotus effect", which is the combination of micro/nano structure roughness and epicuticular waxes that results in reduced contact area between water droplets and a leaf's surface at contact angles exceeding 150 degrees (Jiang *et al*. 2004; Wang *et al*. 2006b). In contrast, the rough microstructure of the veneer traps the air in the porous void and cell lumen of its surface and strongly affects the gas fraction of veneer-liquid interface, which can weaken the interface hydrophilicity (Fig. 6). As illustrated in Fig. 6b, the air fraction decreases as the surfaces roughness decreases by compression treatment. This leads to an increase in the interfacial contact area for the liquid-veneer interface.

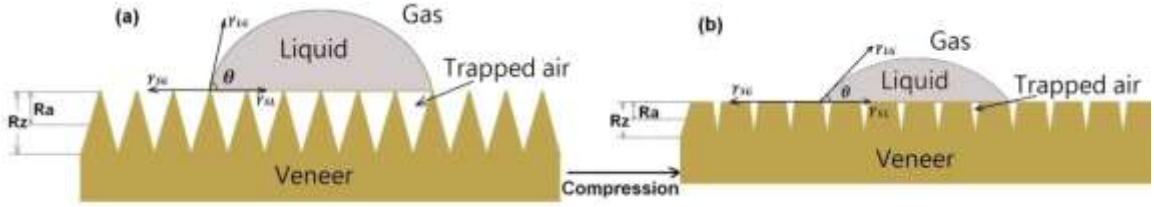


**Fig. 6.** Schematic illustration of wettability of veneer influenced by surface roughness: (a), uncompressed veneer (control); (b), compressed veneer

The relationship between the CA of a liquid droplet on a smooth surface ($\theta_s$) and the CA on its rough surface ($\theta_r$) can be described by the Cassie-Baxter state (Jiang *et al*. 2004; Spori *et al*. 2008):

$$\cos\theta_r = f_1 \cos\theta_s - f_2 \quad (9)$$

where $f_1$ and $f_2$ are the area fractions of solid surface and air in contact with liquid, respectively. According to Eq. 9, the values of CA decrease as the contact area ($f_1$) increases.

Therefore, the SFE of veneer increased by 12% with as little as 11% CR through hot compression. The results are in accordance with a previous states that the CR required for achieving a target 80% contact area is about 10.5% for plywood/LVL

products (Wang *et al* 2006a). Theoretically, an increase in the SFE or wettability will improve the bond quality between veneer surfaces. Furthermore, with improvement in the wettability of veneer surfaces, a low level of glue spread can meet the standard requirements for panels. This not only reduces glue consumption but also shortens the hot pressing time in the production of veneer-based composites.

## CONCLUSIONS

1. The wettability of poplar veneer was improved by hot compression treatment at 120 °C. The values of total SFE increased by 12% at a compression ratio (CR) level of 11%. When the CR of veneer exceeded 11%, the total surface free energy (SFE) increased slightly. The increase in SFE is mainly due to increasing interfacial contact area of the hydrophilic veneer and decreasing hydrophobic air in the liquid-veneer interface as the CR levels increase.
2. A predominant factor regarding the total SFE was surface roughness, while the chemistry change on the veneer surfaces was a secondary and negative factor.
3. With increasing CR, the O/C ratio of the veneer surface decreased, while the C1/C2 ratio increased. This is due to the chemical changes by migration and concentration of extractives on the surface.
4. The work of adhesion for veneer-liquid interaction showed a significant increase with increasing CR of veneer up to 11%. Then, the values increased slightly as the CR increased from 11% to 45%. Nevertheless, the work of adhesion for veneer-hexane interactions remained constant at 36.8 mJ $m^{-2}$ due to the zero CA.
5. Compared to the control, both surface roughness parameters $R_a$ and $R_z$ decreased by 15.6% and 20.6%, respectively, for compressed veneer at a CR level of 11%.

## ACKNOWLEDGMENTS

This work was supported by the National Nature Science Fund of China (No. 31070492) and the Graduate Student Innovation Project of Jiangsu Province (No. CXZZ13_0542).

## REFERENCES CITED

Anshari, B., Guan, Z. W., Kitamori, A., Jung, K., Hassel, I., and Komatsu, K. (2011). "Mechanical and moisture-dependent swelling properties of compressed Japanese cedar," *Constr. Build. Mater*. 25(4), 1718-1725.

Avila, C. B., Escobar, W. G., Cloutier, A., Fang, C., and Carrasco, P. V. (2012). "Densification of wood veneers combined with oil-heat treatment. Part III: Cell wall mechanical properties determined by nanoindentation," *BioResources* 7(2), 1930-2126.

Ayrilmis, N., Dundar, T., Candan, Z., and Akbulut, T. (2009). "Wettability of fire retardant treated laminated veneer lumber (LVL) manufactured from veneers dried at different temperatures," *BioResources* 4(4), 1536-1544.

B46.1 (2002). *Surface Texture, Surface Roughness, Waviness and Lay*, American Society of Mechanical Engineers, New York, USA.

Bao, F., and Liu, S. (2001). "Modeling the relationships between wood properties and quality of veneer and plywood of Chinese plantation poplars," *Wood Fiber Sci.* 33(2), 264-274.

Bekhta, P., Hiziroglu, S., and Shepelyuk, O. (2009). "Properties of plywood manufactured from compressed veneer as building material," *Mater. Design* 30(4), 947-953.

Bekhta, P., Niemz,P., and Sedliacik, J. (2012). "Effect of pre-pressing of veneer on the glueability and properties of veneer-based products," *Eur. J. Wood Prod.* 70(1-3), 99-106.

Büyüksarı, Ü. (2013). "Surface characteristics and hardness of MDF panels laminated with thermally compressed veneer," *Compos. Part B-Eng*. 44(1), 675-678.

Cai, J., Yang, X., Cai, L., and Shi, S. Q. (2013). "Impact of the combination of densification and thermal modification on dimensional stability and hardness of poplar lumber," *Dry. Technol.* 31(10), 1107-1113.

Candan, Z., Hiziroglu, S., and McDonald, A. G. (2010). "Surface quality of thermally compressed Douglas fir veneer," *Mater. Design* 31(7), 3574-3577.

Čern, L., Simončič, B., and Željkob, M. (2008). "The influence of repellent coatings on surface free energy of glass plate and cotton fabric," *Appl. Surf. Sci.* 254(20), 6467-6477.

Diouf, P. N., Stevanovic, T., Cloutier, A., and Fang, C. (2011). "Effects of thermo-hygro-mechanical densification on the surface characteristics of trembling aspen and hybrid poplar wood veneers," *Appl. Surf. Sci.* 257(8), 3558-3564.

Fang, C., Cloutier, A., Blanchet, P., Koubaa, A., and Mariotti, N. (2011). "Densification of wood veneers combined with oil-heat treatment. Part I: Dimensional stability," *BioResources* 6(1), 373-385.

Fang, C., Cloutier, A., Blanchet, P., and Koubaa, A. (2012a). "Densification of wood veneers combined with oil-heat treatment. Part II: Hygroscopicity and mechanical properties," *BioResources* 7(1), 925-935.

Fang, C., Mariotti, N., Cloutier, A., Koubaa, A., and Blanchet, P. (2012b). "Densification of wood veneers by compression combined with heat and steam," *Eur. J. Wood Prod.* 70(1-3), 155-163.

Gardner, D. J. (1996). "Application of the Lifshitz-van der Waals acid-base approach to determine wood surface tension components," *Wood Fiber Sci.* 28(4), 422-428.

Gindl, M., Sinn, G., and Gindl, W. (2001). "A comparison of different methods to calculate the surface free energy of wood using contact angle measurements," *Colloid. Surface. A* 181(1), 279 -287.

Gong, M., Lamason, C., and Li, L. (2010). "Interactive effect of surface densification and post-heat-treatment on aspen wood," *J. Mater. Process. Tech.* 210(2), 293-296.

Good, R. J. (1992). "Contact angle, wetting, and adhesion: A critical review," *J. Adhes. Sci. Technol.* 6(12), 1269-1302.

Hakkou, M., Pétrissans, M., Zoulalian, A., and Gérardin, P. (2005). "Investigation of wood wettability changes during heat treatment on the basis of chemical analysis," *Polym. Degrad. Stabil*. 89(1), 1-5.

Haygreen, J. G., and Daniels, D. H. (1969). "The simultaneous drying and densification of sapwood," *Wood Fiber Sci*. 1(1), 38-53.

Heräjärvi, H. (2009). "Effect of drying technology on aspen wood properties," *Silva Fenn*. 43(3), 433-445.

İmirzi, H. Ö., Ülker, O., and Burdurlu, E. (2014). "Effect of densification temperature and some surfacing technique on the surface roughness of densified Scots pine (*Pinus sylvestris L*.)," *BioResources* 9(1), 191-209.

Inari, G. N., Petrissans, M., Lambert, J., Ehrhardt, J. J., and Gérardin, P. (2006). "XPS characterization of wood chemical composition after heat-treatment," *Surf. Interface Anal*. 38(10), 1336-1342.

Jiang, L., Zhao, Y., and Zhai, J. (2004). "A lotus-leaf-like superhydrophobic surface: A porous microsphere/nanofiber composite film prepared by electrohydrodynamics," *Angew. Chem. Int. Edit.* 43(33), 4338-4340.

Kutnar, A. and Kamke, F. A. (2012). "Compression of wood under saturated steam, superheated steam, and transient conditions at 150 °C, 160 °C, and 170 °C," *Wood Sci. Technol.* 46(1-3), 73-88.

Kutnar, A., Kamke, F. A., Petrič, M., and Sernek, M. (2008). "The influence of viscoelastic thermal compression on the chemistry and surface energetics of wood," *Colloid. Surface. A* 329(1-2), 82-86.

Kutnar, A., Kamke, F. A., and Sernek, M. (2009). "Density profile and morphology of viscoelastic thermal compressed wood," *Wood Sci. Technol.* 43(1-2), 57-68.

Kwok, D. Y., Li, D., and Neumann, A. W. (1994). "Evaluation of the Lifshitz-van der Waals/acid-base approach to determine interfacial tensions," *Langmuir* 10(4), 1323-1328.

Li, W., Zhang, Y., Ruan, Z., and Liu, Y. (2010). "Influence of veneer compression and resin impregnation on the properties of poplar plywood," *China Forest Prod. Ind.* 37(6), 10-13.

Ma, D., Johns, W. E., Dunker, A. K., and Bayoumi, A. E. (1990). "The effect of donor-acceptor interactions on the mechanical properties of wood," *J. Adhes. Sci. Technol.* 4(1), 411-429.

Mahadik, D. B., Rao, A. V., Parale, V. G., Kavale, M. S., Wagh, P. B., Ingale, S. V., and Gupta, S. V. (2011). "Effect of surface composition and roughness on the apparent surface free energy of silica aerogel materials," *Appl. Phys. Lett.* 99(10), 104104.

McConnell, T. E., and Shi, S. Q. (2011). "Surface energy characterization of three partially hydrolyzed hardwood species determined by dynamic contact angle analysis," *J. Adhesion* 87(4), 353-365.

Miller, J. D., Veeramasuneni, S., Drelich, J., Yalamanchili, M. R., and Yamauchi, G. (1996). "Effect of roughness as determined by atomic force microscopy on the wetting properties of PTFE thin films," *Polym. Eng. Sci.* 36(14), 1849-1855.

Mohammed-Ziegler, I., Oszlánczi, Á., Somfai, B., and Hórvölgyi, Z. (2004). "Surface free energy of natural and surface-modified tropical and European wood species," *J. Adhes. Sci. Technol.* 18(6), 687-713.

Mohan, T., Kargl, R., Doliška, A., Vesel, A., Köstler, S., Ribitsch, V., and Stana-Kleinschek, K. (2011). "Wettability and surface composition of partly and fully regenerated cellulose thin films from trimethylsilyl cellulose," *J. Colloid Interf. Sci.* 358(2), 604-610.

Ostrovskaya, L., Podesta, A., Milani, P., and Ralchenko, V. (2003). "Influence of surface morphology on the wettability of cluster-assembled carbon films," *Euro. Phys. Lett*. 63(3), 401-407.

Owens, D. K., and Wendt, R. C. (1969). "Estimation of the surface free energy of polymers," *J. Appl. Polym. Sci.* 13(8), 1741-1747.

Plötze, M., and Niemz, P. (2011). "Porosity and pore size distribution of different wood types as determined by mercury intrusion porosimetry," *Eur. J. Wood Prod.* 69(4), 649-657.

Poncsak, S., Kocaefe, D., Simard, F., and Pichette, A. (2009). "Evolution of extractive composition during thermal treatment of Jack pine," *J. Wood Chem. Technol*. 29(3), 251-264.

Rautkari, L., Properzi, M., Pichelin, F., and Hughes, M. (2010). "Properties and set-recovery of surface densified Norway spruce and European beech," *Wood Sci. Technol.* 44(4), 679-691.

Rossi, D., Rossi, S. Morin, H.,and Bettero, A. (2012). "Within-tree variations in the surface free energy of wood assessed by contact angle analysis," *Wood Sci. Technol.* 46(1-3), 287-298.

Rudawska, A., and Jacniaka, E. (2009). "Analysis for determining surface free energy uncertainty by the Owen-Wendt method," *Int. J. Adhes.* 29(4), 451-457.

Selvakumar, N., Barshilia, H. C., and Rajam, K. S. (2010). "Effect of substrate roughness on the apparent surface free energy of sputter deposited superhydrophobic polytetrafluorethylene coatings: A comparison of experimental data with different theoretical models," *J. Appl. Phys.* 108(1), 013505.

Sernek, M. (2002). "Comparative analysis of inactivated wood surfaces," Ph.D. Thesis, Virginia Polytechnic Institute and State University, USA.

Shen, Q., Nylund, J. and Rosenholm, J. B. (1998). "Estimation of the surface energy and acid-base properties of wood by means of wetting method," *Holzforschung* 52(5), 521-529.

Shen, W., Sheng, Y. J., and Parker, I. H. (1999). "Comparison of the surface energetics data of eucalypt fibers and some polymers obtained by contact angle and inverse gas chromatography methods," *J. Adhes. Sci. Technol.* 13(8), 887-901.

Shi, S. Q., and Gardner D. J. (2001). "Dynamic adhesive wettability of wood," *Wood Fiber Sci.* 33(1), 58-68.

Spori, D. M., Drobek, T., Zürcher, S., Ochsner, M., Sprecher, C., Mühlebach, A., and Spencer, N. D. (2008). "Beyond the lotus effect: Roughness influences on wetting over a wide surface-energy range," *Langmuir* 24(10), 5411-5417.

Tjeerdsma, B. F., and Militz, H. (2005). "Chemical changes in hydrothermal treated wood: FTIR analysis of combined hydrothermal and dry heat-treated wood," *Holz. Roh. Werkst*. 63(2), 101-111.

Van Oss, C. J., Chaudhury, M. K., and Good, R. J. (1987). "Monopolar surfaces," *Adv. Colloid Interf. Sci.* 28(1), 35-64.

Van Oss, C. J., and Giese, R. F. (1995). "The hydrophilicity and hydrophobicity of clay minerals," *Clay. Clay. Miner.* 43(4), 474-477.

Van Oss, C. J., Giese, R. F., Li, Z., Murphy, K., Norris, J., Chaudhury, M. K., and Good, R. J. (1992). "Determination of contact angles and pore sizes of porous media by column and thin layer wicking," *J. Adhes. Sci. Technol.* 6(4), 413-428.

Wålinder, M. E. P. (2002). "Study of Lewis acid-base properties of wood by contact angle analysis," *Holzforschung* 56(4), 363-371.

Wålinder, M. E. P., and Ström, G. (2001). "Measurement of wood wettability by the Wilhelmy method. Part 2. Determination of apparent contact angles," *Holzforschung* 55(1), 33-41.

Wang, B. J., Ellis, S., and Dai, C. (2006a). "Veneer surface roughness and compressibility pertaining to plywood/LVL manufacturing. Part II. Optimum panel densification," *Wood Fiber Sci.* 38(4), 727-735.

Wang, S., Zhu, Y., Xia, F., Xi, J., Wang, N., Feng, L., and Jiang, L. (2006b). "The preparation of a superhydrophilic carbon film from a superhydrophobic lotus leaf," *Carbon* 44(9), 1848-1850.

Wei, P., Wang, B. J., Zhou, D., Dai, C., Wang, Q., and Huang, S. (2013). "Mechanical properties of poplar laminated veneer lumber modified by carbon fiber reinforced polymer," *BioResources* 8(4), 4883-4898.

Wu, S. (1971). "Calculation of interfacial tension in polymer systems," *J. Polym. Sci. C* 34(1), 19-30.

Young, R. A., Rammon, R. M., Kelley, S. S., and Gillespie, R. H. (1982). "Bond formation by wood surface reactions: Part I. Surface-analysis by ESCA," *Wood Sci.* 14(3), 110-119.

Young, T. (1805). "An essay on the cohesion of fluids," *Philosophical Transactions of the Royal Society of London* 95, 65-87.

Zenkiewicz, M. (2007). "Comparative study on the surface free energy of a solid calculated by different methods," *Polym. Test*. 26(1), 14-19.

Zhang, Y., Wang, S., Hosseinaei, O., and Zhou, Z. (2012). "Effects of compressive deformation on wettability and water uptake behavior of poplar," *Forest Prod. J.* 62(6), 450-455.

Zisman, W. A. (1963). "Influence of constitution on adhesion," *Ind. Eng. Chem*. 55(10), 18-38.

Article submitted: December 22, 2013; Peer review completed: March 9, 2014; Revised version received and accepted: March 27, 2014; Published: April 3, 2014.